# Investigation of the Formation Reaction and Structural Characterization of the "Platinum Grignard Reagent" $[Pt(MgCl)_2(THF)_x]$ by Extended X-ray Absorption Fine Structure (EXAFS) and Other Methods

**Lorraine E. Aleandri, Borislav Bogdanović,* Christine Dürr, Sara C. Huckett, Deborah J. Jones, Uwe Kolb, Martin Lagarden, Jacques Rozière,* and Ursula Wilczok**

**Abstract:** The "platinum Grignard reagent" $[Pt(MgCl)_2(THF)_x]$ (**2**), obtained by the reaction of $PtCl_2$ and $Et_2Mg$ in a 1:2 molar ratio, as well as finely divided platinum (Pt*)—a possible intermediate formed during the preparation of **2**—have been investigated by EXAFS spectroscopy at the Pt $L_{III}$ edge. Parallel investigations were carried out on Pt* obtained from $PtCl_2$ and (9,10-dihydro-9,10-anthracenediyl)tris(tetrahydrofuran)magnesium (MgA), and on **2** obtained from Pt*, MgA, and $MgCl_2$. The EXAFS results suggest that Pt* consists of extremely small particles ($\approx 5-11$ Å) with strongly reduced Pt–Pt distances compared to bulk Pt ($\approx 0.09$ Å). The EXAFS spectra of **2** indicate the presence of Mg shells in addition to Pt shells in the Pt environment; Mg atoms are at a bonding distance from Pt atoms (2.78–2.80 Å). These results suggest that **2** consists of very small Pt–Mg clusters and confirm their formation from organomagnesium reagents and $PtCl_2$ or Pt*.

**Keywords**
clusters · EXAFS spectroscopy · Grignard reactions · magnesium · platinum

## Introduction

In recent publications[1] we reported the preparation of a series of novel, so-called inorganic Grignard reagents of general formula $[M(MgCl)_m \cdot (MgCl_2)_p]$ (M = Group 8–10 transition metal; $m = 1, 2, 3$; $p = 0, 1$) and their applications in the synthesis of nano-particulate intermetallics and alloys.

In the preparation of Grignard reagents of palladium (**1**) and platinum (**2**) from the corresponding metal chlorides and diethylmagnesium ($Et_2Mg$), a notable distinction between the reactions leading to **1** and **2** was observed.[1a] Reagents **1** can only be prepared by slowly warming a mixture of $PdCl_2$ and $Et_2Mg$, in a molar ratio of 1:2 in THF, from $-78\,^{\circ}C$ to RT [Eq. (1)]; finely divided palladium (Pd*), prepared from $PdCl_2$ and $Et_2Mg$ under the same conditions [Eq. (1a)], does *not* react

$$PdCl_2 + 2Et_2Mg \xrightarrow[-78\,^{\circ}C \rightarrow RT]{THF} \underset{\mathbf{1}}{[Pd(MgCl)_2](THF)_x} + 2(C_2H_6 + C_2H_4)\uparrow \quad (1)$$

$$PdCl_2 + Et_2Mg \xrightarrow[-78\,^{\circ}C \rightarrow RT]{THF} Pd^*\downarrow + MgCl_2 + 2(C_2H_6 + C_2H_4)\uparrow \xrightarrow[\Delta]{EtMg} \text{no reaction} \quad (1a)$$

with (additional) $Et_2Mg$ and $MgCl_2$ to give **1**. In contrast, **2** can be prepared by both the one-[1a] and the two-step process [Section A, Eqns. (2) and (2a)].

The surprising macroscopic observation that a suspension of Pt* could react with an organometallic reagent ($Et_2Mg$ or EtMgCl) under ambient conditions to generate a soluble bimetallic species [**2**, Eq. (2a)] as well as the possibility that Pt* could be an intermediate in the formation of **2** [Eq. (2)], required verification by spectroscopic methods. In the following we report investigations on the formation reactions and the structural characterization of **2** and of intermediate Pt* by means of NMR and EXAFS[2] spectroscopy (Section A). Parallel investigations on the formation of **2** from $PtCl_2$ and $MgA \cdot 3THF$[3] (Section B) are also described.

[*] Dr. L. E. Aleandri, Prof. B. Bogdanović, Dr. C. Dürr, Dr. S. C. Huckett, Dr. U. Kolb, Dr. M. Lagarden, U. Wilczok
Max-Planck-Institut für Kohlenforschung
Postfach 101353, 45466 Mülheim an der Ruhr (Germany)
FAX: Int. code +(208)306-2980
Dr. D. J. Jones, Prof. J. Rozière
Laboratoire des Agrégats Moléculaires et Matériaux Inorganiques URAC-NRS 79, Université de Montpellier II
F-34095 Montpellier Cedex 5 (France)



0947-6539/97/0310-1710 $ 17.50+.50/0

Table 1. $^1$H NMR study of the reaction of $PtCl_2$ with $Et_2Mg$ (molar ratio 1:2) in [D$_8$]THF [Eq. (2)].

| React. $T$ (°C) | React. $t$ (h) | $T$ $^1$H NMR spectrum (°C) | Chemical shifts $\delta$ $C_2H_4$ | $C_2H_6$ | $CH_2CH_3$ | $CH_2CH_3$ | Intensity ratio of signals $C_2H_4$:$C_2H_6$:$CH_2CH_3$ | Additional (weak) signals $\delta$ |
|---|---|---|---|---|---|---|---|---|
| −78 → −60 | 18 | −60 | 5.39 | 0.83 | 1.16 | −0.85 (−0.72) | 1:1.8:1.5 | 0.57, 0.30 |
| −60 → −20 | 2 | −20 | 5.39 | 0.83 | 1.16 | −0.85 | 1:1.9:0.9 | 0.52 [a] |
| −20 → 0 | 0.5 | 0 | 5.39 | 0.83 | 1.16 | −0.85 | 1:1.8:0.5 | 0.52 [b] |
| RT | 120 | +27 | 5.39 | 0.83 | – | – | 1:3.3:0.0 | – |

[a] Broad signal. [b] Further broadening of the signal.

## Results

**A. Preparation and characterization of 2 and of Pt* from $PtCl_2$ and $Et_2Mg$**: The one-step preparation of **2** [Eq. (2)] has already been reported.[1a, 4]

$$PtCl_2 + 2Et_2Mg \xrightarrow[-78\,^\circ C \rightarrow \text{reflux}]{\text{THF}} \underset{\mathbf{2}}{[Pt(MgCl)_2(THF)_x]} + 2(C_2H_6 + C_2H_4)\uparrow \quad (2)$$

*$^1$H NMR spectroscopy*: The formation of **2** in [D$_8$]THF [Eq. (2)] with a temperature gradient from −78 to +27° was monitored by $^1$H NMR spectroscopy (Table 1; experiment 3.1, i.e., Table 3, experiment 1). The spectrum recorded at −60 °C already revealed the presence of $C_2H_4$ and $C_2H_6$. In addition to signals from EtMg ($\delta = 1.16$ and −0.85, shoulder at −0.72), weak multiplets at $\delta = 0.57$ and 0.30 were observed. At −20 °C, the signals of $C_2H_4$ and $C_2H_6$ had increased, while those of EtMg had decreased. The multiplets at $\delta = 0.57$ and 0.30 were no longer present, but a broad signal appeared at $\delta = 0.52$. At RT, only signals of $C_2H_6$ and $C_2H_4$ were observed.[5, 6] The evidence from $^1$H NMR spectroscopy thus confirms the stoichiometry of the reaction given in Equation (2), and in contrast to the EXAFS experiment (see below), the reaction at RT reached completion in this experiment.

*$^{195}$Pt and $^{25}$Mg NMR spectroscopy*: No $^{195}$Pt signal could be detected in a solution of **2** in [D$_8$]THF;[7] however, there was a broad $^{25}$Mg signal (780 Hz width) at $\delta = 20$. This signal is shifted downfield and is broader than that observed for $MgCl_2$ in [D$_8$]THF ($\delta = 16.4$, 350 Hz width).[8] These differences with respect to $MgCl_2$ cannot be explained precisely (coordination of Pt to Mg, changes in the coordination sphere of Mg, etc.), however, the $^{25}$Mg signal detected points to the presence of Mg–Cl bonds in **2**.

*Two-step preparation of 2* [Eq. (2a); experiment 3.2]: $PtCl_2$ reacts with $Et_2Mg$ in the molar ratio 1:1 at −70 °C → RT with evolution of a gaseous mixture of $C_2H_6$ and $C_2H_4$ to produce a black precipitate—presumably Pt* [Eq. (2a)]. At this stage of

$$PtCl_2 + Et_2Mg \xrightarrow[-78\,^\circ C \rightarrow RT]{\text{THF}} Pt^*\downarrow + MgCl_2 + (C_2H_6 + C_2H_4)\uparrow \xrightarrow[-C_2H_6-C_2H_4]{Et_2Mg/\Delta} \mathbf{2} \quad (2a)$$

the reaction, the absence of any $Et_2Mg$ or EtMgCl in the THF solution was proved by $^1$H NMR spectroscopy. After addition of a second equivalent of $Et_2Mg$ and stirring of the suspension for 3 h at RT, *dissolution of the black precipitate* was observed. In order to complete the reaction, it was necessary to reflux the reaction mixture for 1–2 h, whereby evolution of a $C_2H_6/C_2H_4$ mixture was observed once again and the second equivalent of $Et_2Mg$ was completely consumed ($^1$H NMR spectroscopy). The resulting solution of **2** was free of any Pt* precipitate.

*EXAFS spectroscopy*: The environment around Pt in **2**, prepared according to Equation (2) (after heating the reaction mixture to reflux, experiment 3.4), as well as that in the intermediate product (prior to refluxing, experiment 3.3) was examined by EXAFS spectroscopy. The spectra were recorded in solution (THF) and in the amorphous solid state, obtained from the evaporation of the solutions to dryness under vacuum. Two types of EXAFS analysis were undertaken: firstly, a conventional curve-fitting procedure in reciprocal space by means of a single scattering formalism, and secondly, modeling of the experimental EXAFS function with functions calculated for various cluster species with the inclusion of multiple scattering pathways.

The results from the curve-fitting procedure indicate that the environment around Pt in **2** (Table 2, Figure 2b) includes 4.0(9) Pt atoms at 2.70(2) Å and 1.8(6) Mg at 2.80(2) Å. This suggests the existence of bimetallic Pt–Mg clusters. Thus, the coordination sphere around Pt in **2** is very different from that found for Ti in the Ti Grignard reagent $[Ti(MgCl)_2(THF)_y]$, in which no Ti neighbors[9] were found. Surprisingly, the environment around Pt in the intermediate (Table 2, Figure 2a) does not correspond to an organochloro–Pt derivative[6] but is characteristic of very small Pt clusters (cf. Section B): 5.5(7) Pt neighbors at 2.68(6) Å with 0.5(6) oxygen atoms (from THF) at 2.03(9) Å. This suggests that the generation of the platinum Grignard reagent **2** proceeds via very small Pt particles. However, nothing higher than the second cumulants were included in the fit. This conventional method has a limitation in deriving structural information on a system composed of very small particles: the absence of any cumulants higher than the second ones may cause the determined Pt–Pt distance to be shifted to a smaller value (estimated error 0.015 Å),[10] and $N$ may be underestimated if the distribution of distances is non-Gaussian. This only affects the absolute value of the determined bond length, but not its interpretation in this paper. The difference between the EXAFS spectra of **2** and of the intermediate Pt* (Figure 2a,b) is noteworthy: the presence of a Mg shell in **2** causes a characteristic dip in the first oscillation near 6 Å$^{-1}$, this is not observed in the Pt* spectrum.

**B. Investigation of the reaction of $PtCl_2$ with 9,10-dihydro-9,10-anthracenediylmagnesium·3THF (MgA)**: In the reaction of $PdCl_2$ with MgA in THF (molar ratio 1:2 or higher) only solid products are formed.[11] $PtCl_2$, on the other hand, reacted with MgA in the molar ratio 1:2 to afford **2** [Eq. (3)].[3, 11] The pres-

  0947-6539/97/0310-1711 $ 17.50+.50/0 

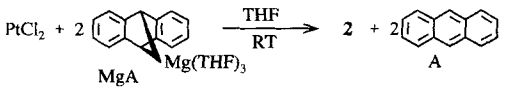


(3)

ence of *free* anthracene in the THF solution following the reaction was verified by IR and NMR spectroscopy, and GC analysis (experiment 4.1).

The preparation of **2** from MgA [Eq. (3)] could also be conducted in two steps, that is, *consecutive* addition of the first and of the second equivalent of MgA to $PtCl_2$; after the reaction of $PtCl_2$ with one equivalent of MgA, a fine black precipitate of Pt* (see below) was observed, which dissolved upon addition of the second equivalent of MgA [Eq. (3a); experiment 4.2].

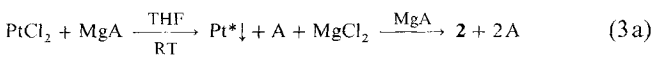


(3a)

It is remarkable that Pt*, even when isolated by filtration as an X-ray amorphous powder (experiments 5.1 and 5.2), still possesses the ability to react with MgA and $MgCl_2$ to afford **2** [Eq. (4); experiments 6.1 and 6.2]. The reaction of the isolated Pt* with MgA and $MgCl_2$ to **2** [Eq. (4)] was monitored by removing samples directly from the reaction mixture and then determining the ratio of anthracene/9,10-dihydroanthracene (DHA) in the hydrolyzed samples by gas chromatography. As can be seen in Figure 1 (*, □; experiment 6.3), at RT the reaction is virtually complete after ca. 15 minutes. In the absence of Pt* (■, ¦) or in the presence of commercial Pt black (×, ◇), only a minor quantity of anthracene[12] was liberated from MgA under the same conditions.

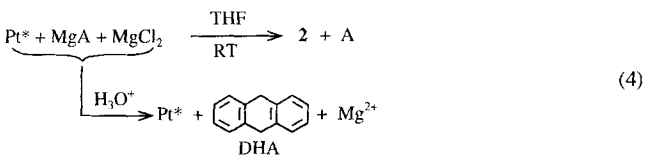


(4)

*EXAFS spectroscopy*: Both the isolated Pt* (experiment 5.1) and **2**, resulting from the reaction of the isolated Pt* with $MgCl_2$ and MgA [Eq. (4); experiment 6.1], were examined by EXAFS spectroscopy (Table 2, Figures 2c,d). Curve fitting showed Pt* to have 6.3(9) Pt neighbors at 2.68(4) Å, a distance that is 0.09 Å shorter than that in bulk platinum (2.77 Å). In addition,

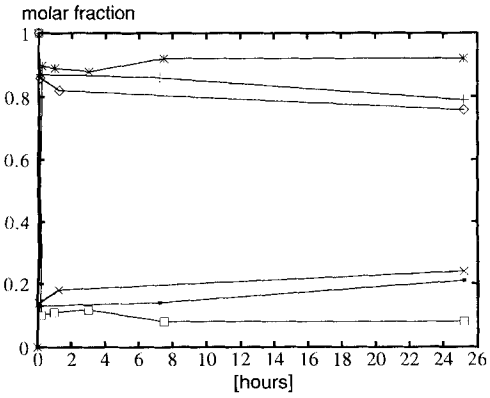


Figure 1. The progression of the reaction of Pt* with (9,10-dihydro-9,10-anthracenediyl)tris(tetrahydrofuran)magnesium (MgA) and $MgCl_2$ to produce the "platinum Grignard reagent" **2** [Eq. (4)]: (*) increase in the concentration of anthracene (A) with time; (□) decrease in the concentration of 9,10-dihydroanthracene (DHA) with time. Control experiment in the absence of Pt*: (■) A, (¦) DHA. Pt black used instead of Pt*: (×) A, (◇) DHA.

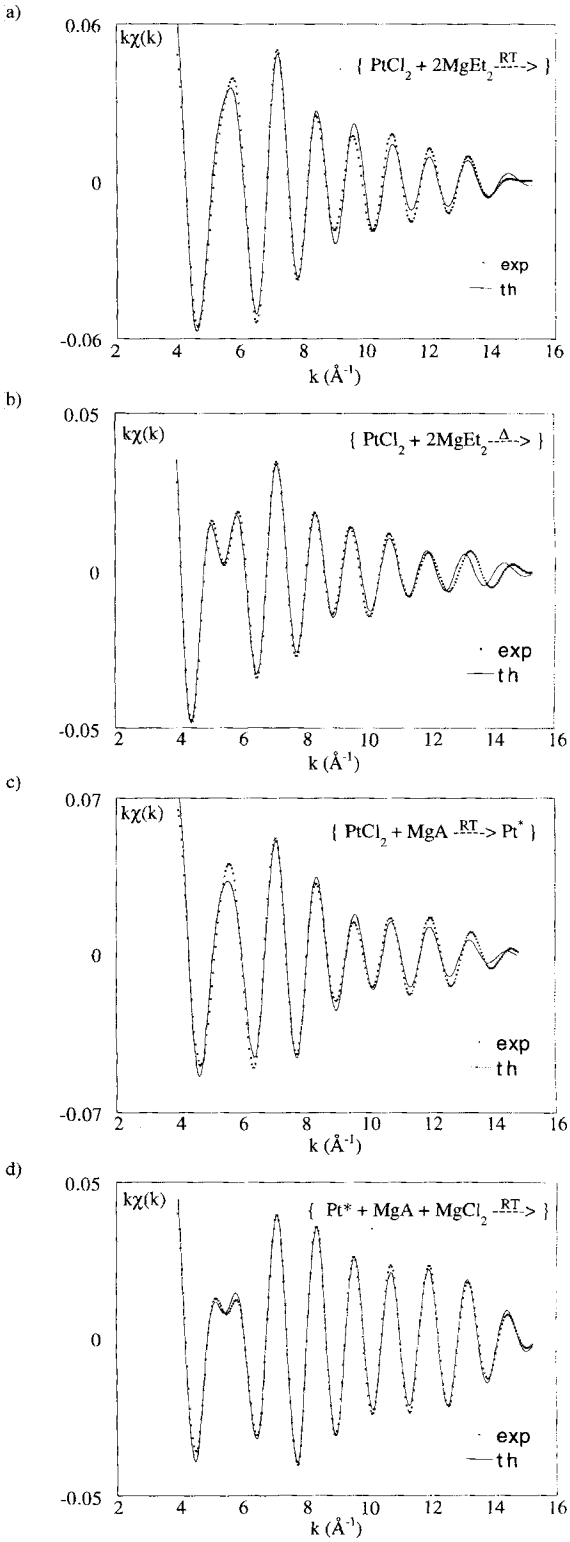


Figure 2. Fits for the back-transformations for a) the intermediate from reaction between $PtCl_2$ and $Et_2Mg$ at RT [Eq. (2a); two shells Pt–O, Pt–Pt]; b) complex **2** from the reaction between $PtCl_2$ and $Et_2Mg$ after refluxing [Eq. (2); two shells Pt–Mg, Pt–Pt]; c) Pt* generated from $PtCl_2$ and MgA [Eq. (3a); two shells Pt–Pt and Pt–C]; d) complex **2** generated from Pt*, MgA, and $MgCl_2$ [Eq. (4); two shells Pt–Mg, Pt–Pt].



0947-6539/97/0310-1712 $ 17.50+.50/0 *Chem. Eur. J.* **1997**, *3*, No. 10

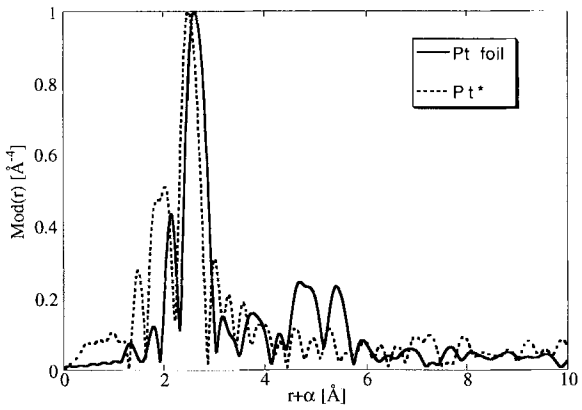


Figure 3. Fourier-transformed $\chi(k)k^3$ functions of Pt foil (solid line) and Pt* (dashed line). The heights of the first peak were scaled to 1.0 for better comparison. In the Pt foil, more distant atom shells can be seen between $R+\alpha = 4$–6 Å.

Table 2. Structural parameters derived from EXAFS spectroscopy for Pt* ($Et_2Mg$) [Eq. (2a)], **2** ($Et_2Mg$) [Eq. (2)], Pt* (MgA) [Eq. (3a)], and **2** (MgA) [Eq. (4)].

| Pt species | Shell | N [a] | $R_{exp}$ [b] (Å) | Res. [c] (%) |
|---|---|---|---|---|
| Pt* ($Et_2Mg$) | Pt | 5.5(7) | 2.68(6) | 1 |
| | Mg | ? | ? | |
| | C | – | – | |
| | O | 0.5(6) | 2.03(9) | |
| **2** ($Et_2Mg$) | Pt | 4.0(9) | 2.70(2) | 2 |
| | Mg | 1.8(6) | 2.80(2) | |
| | C | – | – | |
| | O | 0.4(?) | 2.08(?) | |
| Pt* (MgA) | Pt | 6.3(9) | 2.68(4) | 2 |
| | Mg | – | – | |
| | C | 0.4(9) | 2.18(7) | |
| | O | – | – | |
| **2** (MgA) | Pt | 3.8(9) | 2.69(1) | 3 |
| | Mg | 1.0(4) | 2.78(5) | |
| | C | – | – | |
| | O | – | | |

[a] Number of atoms in the shell. [b] Distance from the Pt absorber. [c] Deviation of the experimental spectrum from the theoretical one as defined by Res. = $\sum_k(\chi_{exp} - \chi_{calcd})^2/\sum_k\chi^2_{exp}$. PtMg alloy was used as a reference substance (Pt–Mg distance: 2.73 Å). Ref.: L. E. Aleandri, B. Bogdanović, U. Wilczok, D. Noreus, G. Block, *Z. Phys. Chem.* **1994**, *185*, 131.

an increase in low $R$ intensity in the Fourier transform of Pt* relative to Pt foil (Figure 3) suggests a shell of light-weight atoms. This contribution could originate from anthracene in Pt*, the presence of which has also been demonstrated by GC experiments (experiments 5.1 and 5.2). In the final fit, 0.4(9) carbon atoms were refined at a distance of 2.18(7) Å from platinum.

After conversion with MgA and $MgCl_2$ into the THF-soluble Pt–Grignard system [**2**, Eq. (7); experiment 6.1] analysis of the EXAFS data (Table 2 and Figure 2d) is compatible with 3.8(9) Pt neighbors at 2.69(1) Å and 1.0(4) Mg at 2.78(5) Å, which is close to the sum of the Pauling radii of the metal atoms (2.73 Å). It should be mentioned here that the Pt–Mg distance in a reference PtMg alloy is 2.73 Å. Once again, a dip in the oscillation near 6 Å is observed. These results tend to confirm (cf. Section A) the formation of bimetallic Pt–Mg nano-sized particles or clusters from Pt*.

## Discussion

Both the low number of Pt neighbors (6.3(9)) in isolated Pt* and, more particularly, the Pt–Pt bond length shortened by 0.09 Å compared to bulk platinum [Eq. (3a); Table 2], are compatible with the existence of extremely small Pt particles. The same holds true for the Pt* intermediate formed from $PtCl_2$ and $Et_2Mg$ [Eq. (2a); Table 2].

The effect of size on the lattice parameter in small particles is well known.[13, 14] Similar Pt–Pt distances (2.68 and 2.66 Å) and similar values for the number of Pt neighbors ($5.4 \pm 0.6$ and $5.7 \pm 0.6$) to those found here for Pt* have been reported[15] for a 1 wt% $Pt/Al_2O_3$ catalyst before and after reaction with *n*-heptane. These clusters were approximately 7 Å in size.[16] In contrast, larger Pt colloids with a particle size of ca. 26 Å and an average coordination number of 11.2 show a contraction of the Pt–Pt distance of only 0.01 Å.[17] In all cases, the derived structural data may reflect a distribution of distances in particles of the same size, a single distance in particles of nonuniform size, or indeed a distribution of distances in particles of different sizes. The number of first-shell distances also depends on the structural type, for example, a single distance is found for fcc and two for a centered icosahedron. Small metal particles are known to adopt well-defined structural types, with cuboctahedral (fcc), icosahedral, or decahedral morphologies being common. It is generally accepted that the fcc structure is progressively more stable as the radius of the particle increases from 7 to 12 Å.[13, 16, 18]

The "magic numbers" for metal clusters with closed shells based on the fcc structure are 13, 55, and 177, while those based on a centered icosahedral structure are 13, 55, and 147.[19] For the former, the average coordination numbers are 5.54, 7.0, and 9.0 atoms for clusters with 13, 55, and 177 atoms, respectively. In a centered icosahedron, two types of nearest-neighbor distances exist: $R_R$, the radial distance between atoms of difference coordination shells, and $R_T$, which corresponds to the distance between atoms of the same shell, whereby $R_T = 1.0561\ R_R$.[20] In order to gain a better understanding of the type of arrangement adopted by Pt*, we calculated the total $\chi(k)k^1$ function of platinum clusters with 13, 55, and 177 atoms for an fcc structure,[21] and with 13 and 55 atoms for clusters with an icosahedral structure,[22] and then compared them with the experimental EXAFS of Pt*. The theoretical $\chi(k)k^1$ function of idealized platinum clusters [fcc structure, $a = 3.7767$ Å (in bulk Pt, $a = 3.924$ Å)] and a centered icosahedral structure with $R_T = 2.67$ Å were calculated by using the program FEFF 6.[23] The theoretical $\chi(k)k^1$ function was calculated for each atom of the cluster by means of the correlated Debye model[24] ($T = 77$ K; Debye temperature = 100 K[25]). The total $\chi(k)k^1$ function was calculated as the average of all the single functions. These functions, and the (nonfiltered) experimental $\chi(k)k^1$ function of isolated Pt* are compared in Figure 4. It can be seen that a characteristic feature (marked with an asterisk in Figure 4), which is caused by multiple scattering, is not present in the $\chi(k)k^1$ functions of the $Pt_{13}$ clusters calculated on the basis of either the fcc or the icosahedral structures. However, this feature does appear in the $\chi(k)k^1$ functions of both the $Pt_{55}$ and the $Pt_{177}$ fcc clusters. For the icosahedral clusters, the presence of two unresolved bond lengths $R_R$ and $R_T$, corresponding to the radial and tangential

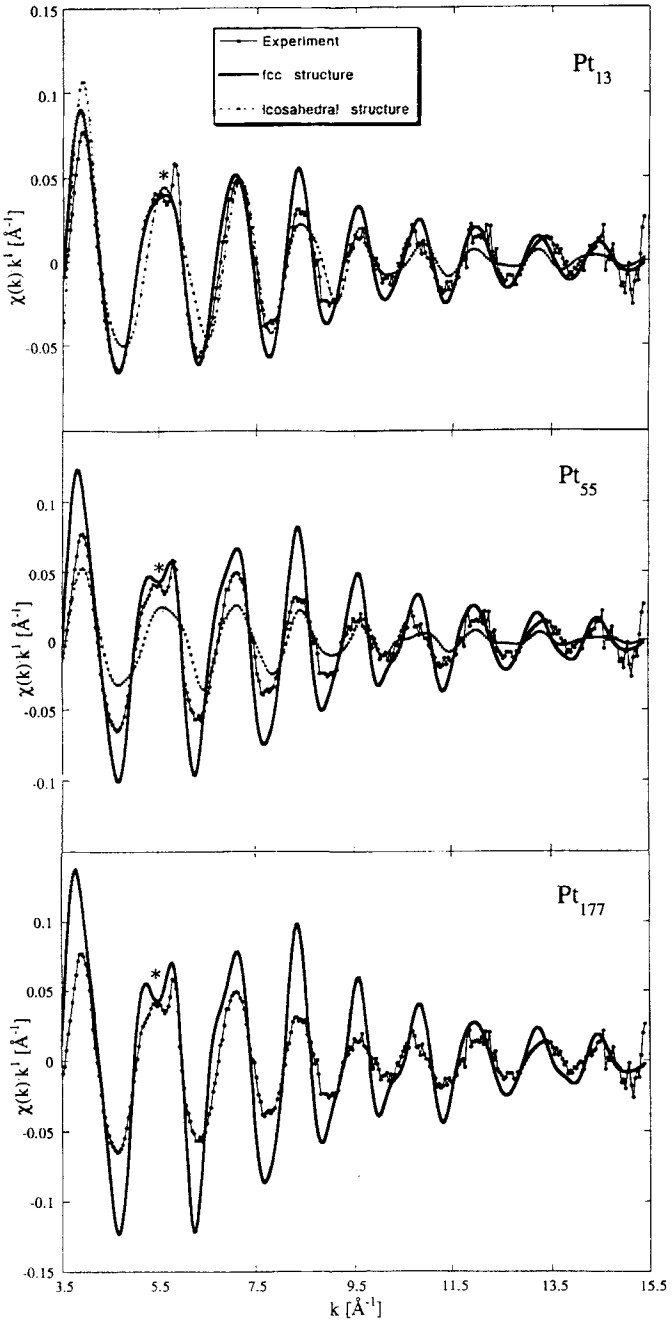


Figure 4. Calculated $\chi(k)k^1$ functions of $Pt_{13}$, $Pt_{55}$, and $Pt_{177}$ (fcc structure, $a$ = 3.7767 Å) and of $Pt_{13}$ and $Pt_{55}$ (icosahedral structure, $R_T$ = 2.67 Å) compared to the non-filtered experimental $\chi(k)k^1$ function of Pt*. The asterisk indicates the characteristic feature between 5 and 6 $Å^{-1}$ (see text).

distances, causes a reduction in the calculated EXAFS amplitude (Figure 4, middle).

Various attempts were made to fit the experimental spectrum of Pt* to the calculated functions of fcc $Pt_{55}$ and icosahedral $Pt_{55}$. The presence of $Pt_{177}$ was not considered at this stage, since the average coordination number in such a cluster is significantly higher than that observed for Pt*. The best agreement is shown in Figure 5, where the experimental $\chi(k)k^1$ spectrum has been fitted with contributions from the calculated functions of fcc (40%) and icosahedral (60%) $Pt_{55}$ clusters. This result, together with the known effect of size on lattice

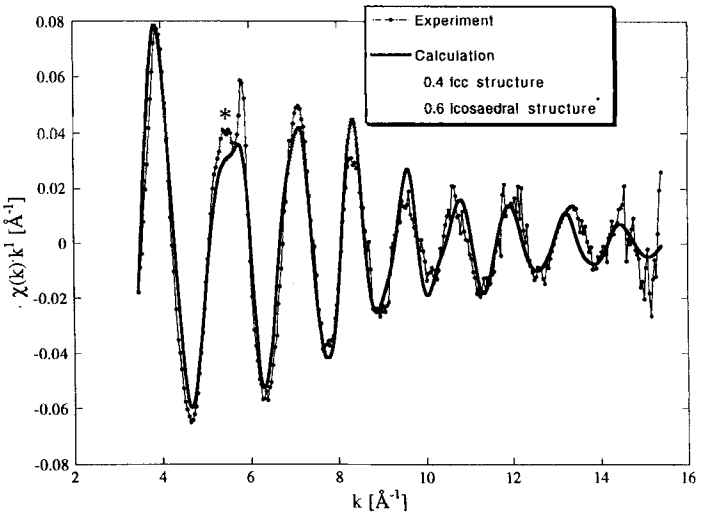


Figure 5. Experimental $\chi(k)k^1$ functions of Pt* fitted with the calculated functions of $Pt_{55}$ with fcc and isocahedral structure. The asterisk indicates the characteristic feature between 5 and 6 $Å^{-1}$ (see text). If the contribution from a carbon backscatterer is taken into account, then the ratio for the best agreement is 0.41 (fcc structure), 0.51 (icosahedral structure), and 0.08 (contribution of a carbon backscatterer).

parameters in small particles, leads to the conclusion that the observed clusters have a particle size close to 55 atoms and display both fcc and icosahedral structures.

In the Fourier-transformed $\chi(k)k^3$ functions of Pt foil and Pt* (Figure 3), it can be seen that the main peak (Pt–Pt distance) is shifted to a lower $R+\alpha$ value for the latter. Furthermore, there is an additional maximum at $R+\alpha = 1.8$ Å, which is attributed to a platinum–carbon contribution in the curve fitting above. Satisfactory agreement in simulations including multiple scattering was obtained without inclusion of a carbon back-scatterer, its contribution to the total $\chi(k)k^3$ function being very small.

The experimental (non-filtered) $\chi(k)k^1$ function of the $[Pt(MgCl)_2(THF)_x]$ sample [**2**, Eq. (4)], when compared to the corresponding function of Pt* (Figure 6), displays a broader and more marked dip between 5 and 6 $Å^{-1}$ with a smaller ampli-

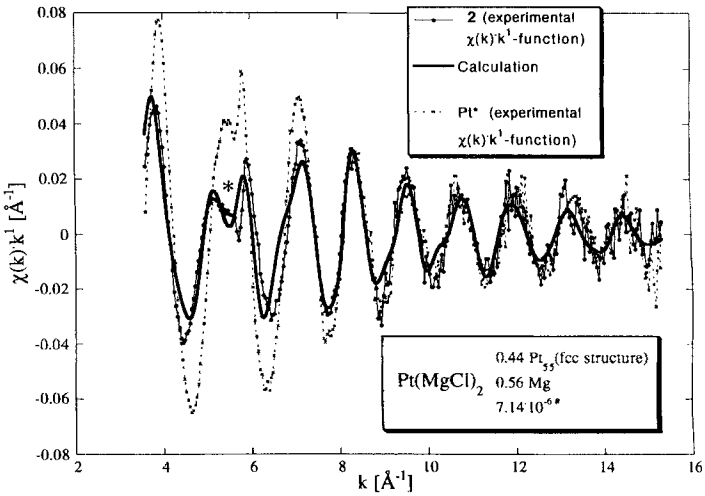


Figure 6. Calculated $\chi(k)k^1$ functions of $Pt_{55}$ (fcc structure, $a$ = 3.7767 Å) with an overlay of a Pt–Mg contribution (distance: 2.70 Å, single scattering only) compared to the experimental $\chi(k)k^1$ function of complex **2** [Eq. (7)]. The asterisk indicates the "dip" between 5 and 6 $Å^{-1}$ (see text).



0947-6539/97/0310-1714 $ 17.50+.50/0 Chem. Eur. J. 1997, 3, No. 10

tude. This dip cannot be reproduced by the $\chi(k)k^1$ function of a simple platinum cluster model similar to those above, or by the sum of such a function and the function of a carbon back-scatterer. However, in agreement with the results of the curve-fitting procedure, the experimental functions can be reproduced with satisfactory agreement by overlaying the $\chi(k)k^1$ function of a $Pt_{55}$ cluster (fcc structure, multiple scattering taken into consideration) with the $\chi(k)k^1$ function of a Pt–Mg absorber–backscatterer pair (single scattering only). This result is shown in Figure 6.

Furthermore, if the experimental $\chi(k)k^1$ function is fitted with the functions of $Pt_{55}$ with fcc and icosahedral structures and an overlay of a Pt–Mg contribution, then the following results are found: 38% $Pt_{55}$ (fcc structure), 12% $Pt_{55}$ (icosahedral structure), and 50% Pt–Mg contribution; sum of standard deviation = $6.79 \times 10^{-6}$.

## Conclusion

EXAFS spectroscopy at the Pt $L_{III}$ edge has provided strong evidence that suspensions of Pt particles (Pt*), prepared by reduction of $PtCl_2$ with $Et_2Mg$ or MgA in THF, react with (additional amounts of) $Et_2Mg$ or MgA and $MgCl_2$ to produce the THF-soluble "platinum Grignard reagent" **2** [Eqs. (2a) and (3a)]. Thus, Pt* is a probable intermediate in the formation of **2** from $PtCl_2$ and $Et_2Mg$ or MgA [Eqs. (2) and (3)].

The results from the analysis of the EXAFS data suggest that the Pt* particles are extremely small (5–11 Å). We have demonstrated that the experimental EXAFS of Pt* can be reproduced more accurately by a combination of the calculated functions of fcc- and icosahedral-structured $Pt_{55}$ than by the use of either of these functions alone. Multiple scattering calculations show a clear difference in the predicted EXAFS of the two types of structure (fcc and icosahedral). This would indicate that, if the particles have a reasonably narrow distribution of size, the nuclearity is close to 55. This cluster is denoted here as "$Pt_{55}$", which is the closest "magic number" to the size envisaged, although any claim that this is the only aggregate present is beyond the limits of this EXAFS analysis. Stabilization of $Ti^0$ particles of comparable size (8 Å) by THF has recently been demonstrated by Bönnemann, Hormes et al.[27] In the present work, both the THF and/or anthracene present in the systems could prevent Pt* particles from agglomerating.

The EXAFS spectra of **2**, prepared with either $Et_2Mg$ or MgA, indicate the presence of both Pt and Mg shells, with Mg atoms at a bonding distance from platinum (2.78–2.80 Å). This result is compatible with the existence of Pt–Mg clusters, the structural arrangement of which can be rationalized in terms of an essentially $Pt_{55}$-like core with $MgCl(THF)_x$ groups on the surface.[28] Total coverage of an fcc "$Pt_{55}$" cluster by magnesium (which is of similar metallic radius) would add a surface shell of 122 magnesium atoms. This value is very close to that determined experimentally in $[Pt(MgCl)_2(THF)_x]$, which is independent confirmation that the core is of a size close to $Pt_{55}$. Some of this magnesium can be removed chemically to give a soluble Pt–Mg system.[28] There is an apparent change in the proportion of fcc- and icosahedral-type structures observed by EXAFS upon formation of $[Pt(MgCl)_2(THF)_x]$ from Pt*.

The phenomenon of dissolution of Pt* suspensions by the formation of the "platinum Grignard reagent" **2** [Eqs. (2a) and (3a)] is a novel example, which demonstrates the extremely high reactivity of nanosized metal particles. Related processes are, for instance, the deposition of Cu on the surface of colloidal Pt particles and the dissolution of Cu in the Pd matrix studied by Bradley et al.,[29] the segregation of bimetallic clusters of immiscible metals (Fe–Mg) investigated by Klabunde et al.,[30] and Basset's surface organometallic chemistry used for the preparation of well-defined Rh–Sn catalysts.[31]

## Experimental Section

The NMR spectra were recorded on a Bruker WH-400 spectrometer.

X-ray absorption spectra were recorded at the Pt $L_{III}$-edge (11 564 eV) on the XAS1 spectrometer (calibrated with a 4 μm Pt foil) at LURE, operating at 1.85 GeV and ≈300 mA. Spectra of $[Pt(MgCl)_2 \cdot (THF)_x]$ complexes, Pt*, crystalline MgPt (HgMn structure), and Pt foil were recorded under identical conditions in a transmission mode with a channel-cut Si(331) monochromator. Spectra were recorded between 11 400 and 12 500 eV in three energy regions in steps of 5 eV in the pre- and post-edge zones and of 2 eV on the edge, using Ar-filled ionization chambers as detectors. Powdered materials were sampled as paraffin oil mulls, prepared under Ar and pressed between the Parafilm windows of stainless steel holders. Sampling of complex solutions was performed in a cell with Mylar windows and with an adjustable path length.[32] All data analyses were performed with the programs developed by Michalowicz[33] (linear pre-edge function and 5–6th order spline polynomial for normalization/background removal). The resulting EXAFS ($\chi(k)$ versus $k$) spectra were Fourier-transformed over a range of typically 2.5–15 $Å^{-1}$ (Hamming window, $k^3$ weighting). Curve-fitting procedures were applied to Fourier-filtered spectra back-transformed to reciprocal space by systematically varying the coordination number $N_i$ (fixed at crystallographic values for reference compounds), the Debye-Waller factor $\sigma_i$, and $R_i$, the distance of the $i$th shell of atoms from the absorber. The spectra of crystalline compounds served as models in the definition of the changes in $E_o$ and the photoelectron mean free path for each type of atom shell when the ab initio phase and amplitude functions of McKale[34] were employed. The $\sigma$ values for each individual shell in the models, as well as in the solid samples, were close to 0.06 Å.

**Analyses:** Elemental analyses and atomic absorption measurements (AAS) of aqueous $Pt^{2+}$ solutions: Dornis and Kolbe, Mülheim an der Ruhr.

**Materials:** Anhydrous $PtCl_2$ (Degussa) was dried under high vacuum and stored under Ar. Pt black: Heraeus. $Et_2Mg$ was prepared and analyzed as previously described.[1a] THF was refluxed for several hours over MgA[35] and subsequently distilled under Ar. All reactions with air-sensitive materials were performed under a dry Ar atmosphere. Vacuum = 0.1–0.2 mbar; high vacuum = $10^{-3}$–$10^{-5}$ mbar.

**Investigation of the reaction represented by Equation (2) by means of $^1$H NMR spectroscopy (Table 3, experiment 1):** A solution of $Et_2Mg$ (17.5 mg, 0.21 mmol) in [$D_8$]THF (1.3 mL) was cooled to −78 °C and transferred under Ar into an NMR tube (5 mm diameter) containing $PtCl_2$ (26.9 mg, 0.10 mmol) at −78 °C. The tube was sealed and stored at −78 °C for 18 h until the first $^1$H NMR spectrum was recorded at −60 °C. The spectra at −20 °C and 0 °C were recorded after a warming period of 2 h and of a further 0.5 h, respectively. The final spectrum at 27 °C was recorded after the tube had been stored for 5 d at RT. The results of the investigation are summarized in Table 1.

**Preparation of 2 by successive addition of the first and the second mol of $Et_2Mg$ per mol of $PtCl_2$ (Table 3, experiment 2):** To a stirred solution of $Et_2Mg$ (97.7% purity, 0.6089 g, 7.23 mmol) in THF (50 mL) was added at −70 °C $PtCl_2$ (1.9252 g, 7.23 mmol) in small portions. The temperature of the reaction mixture and the evolution of gas during the reaction were registered by a thermocouple and an automatic gas burette[36] connected to the reaction flask. The reaction mixture was stirred constantly for 18 h, then it was allowed to gradually warm to RT and was subsequently stirred at RT for a

  0947-6539/97/0310-1715 $ 17.50+.50/0 

Table 3. Investigation of the reaction of $PtCl_2$ with $Et_2Mg$ (molar ratio 1:2) or EtMgCl (molar ratio 1:4).

| Expt | $PtCl_2$ (g) (mmol) | Mg reag. (mmol) | Pt:Mg ratio | THF (mL) | React. $T$ (°C)/ react. $t$ (h) | Mol evolved gas/ mol of $PtCl_2$ [a] | Solid (g) | Mol of gas/mol Pt during hydrol. | Method of reaction investig. |
|---|---|---|---|---|---|---|---|---|---|
| 1 | 0.027 (0.10) | $Et_2Mg$ (0.21) | 1:2 | 1.3 | see Table 1 | | | | $^1H$ NMR, see Table 1 |
| 2 | 1.93 (7.23) | $Et_2Mg$ (7.23) | 1:1 | 60 | $-70 \rightarrow$ RT/18 RT/2 3 | 1.11 $C_2H_6$ 0.35 $C_2H_4$ | | | $^1H$ NMR |
| | | $Et_2Mg$ (7.35) | 1:1 | 10 | RT/3 RF [b]/1.5 RT/24 | 0.80 $C_2H_6$ 1.51 $C_2H_4$ | 0.0 | | $^1H$ NMR |
| 3 | 0.68 (2.55) | $Et_2Mg$ (4.61) | 1:1.8 | 40 | $-78 \rightarrow$ RT/1 RT/72 | n.d. [c] | | 0.18 $C_2H_6$ 0.02 $H_2$ | EXAFS, see Table 2 |
| 4 [d] | 2.77 (10.4) | $Et_2Mg$ (21.1) | 1:2 | 100 | $-70$/19 $-70 \rightarrow$ RT/12.5 RT/85 | 1.3 $C_2H_6$ 1.2 $C_2H_4$ | | 1.1 $C_2H_6$ | |
| | | | | | RF [b]/2 | 0.25 $C_2H_6$, 0.35 $C_2H_4$ | 0.0 | 0.29 $H_2$, 0.2 $C_2H_6$ | EXAFS, Table 2 |
| 5 | 1.36 (5.11) | EtMgCl (20.5) | 1:4 | 60 | $-70$/12 $-70 \rightarrow$ RT/11 RT/20 RF [b]/2.5 | 1.57 $C_2H_6$ 2.19 $C_2H_4$ | 0.0 | 0.44 $H_2$ 0.04 $C_2H_6$ | Precip. of $MgCl_2$ by $C_4H_8O_2$ |

[a] During the reaction. [b] THF reflux temperature. [c] Not determined. [d] Compiled from ref. [1a], expt 3.1.

further 2–3 h. At this stage, the reaction mixture had become deep brown with a black precipitate. The amount of gas evolved was determined as described in experiment 2.1 of ref. [1a] and was found to be 1.11 $C_2H_6$ and 0.35 $C_2H_4$/Pt. A portion (2 mL) of the solution was evaporated under vacuum and the residue dissolved in [$D_8$]THF. According to the $^1H$ NMR spectrum, the solution was free of $Et_2Mg$ or EtMgCl. Subsequently, a solution of $Et_2Mg$ (0.6192 g, 7.35 mmol) in THF (10 mL) was added to the THF suspension and the mixture stirred at RT for 3 h, *during which time dissolution of the black precipitate was observed.* In order to complete the reaction, the mixture was refluxed for $1^1/_2$ h and then stirred at RT for further 24 h. The amount of gas evolved after reaction with the second mol of $Et_2Mg$/mol of $PtCl_2$ (cf. above) was found to be 0.80 $C_2H_6$ and 1.51 $C_2H_4$/Pt. The resulting deep brown solution was free of any precipitate and contained no $Et_2Mg$ or EtMgCl ($^1H$ NMR spectroscopy). The THF solution was found to contain $Mg^{2+}$ (13.9 mmol) and Cl (13.0 mmol).

**Investigation of the reaction product $PtMg_2Cl_2C_{10.8}H_{22.9}$, obtained from $PtCl_2$ and $Et_2Mg$ (molar ratio 1:1.8) at RT, by means of EXAFS spectroscopy (Table 3, experiment 3):** $PtCl_2$ (0.6774 g, 2.55 mmol) was suspended in THF (20 mL) and $Et_2Mg$ (28.8% Mg, 88.5% Et groups; 0.4284 g, 4.61 mmol) was dissolved in THF (20 mL) and each were cooled to $-78$ °C. The $PtCl_2$ suspension was then added to the $Et_2Mg$ solution and the resulting suspension then warmed to RT over a period of 1 h, stirred at RT for a further 72 h, and the solvent then removed under vacuum. Elemental analysis of the solid residue (1.19 g): Pt 35.52, Mg 8.84, Cl 13.04, C 23.52, H 4.17% ($PtMg_2Cl_2C_{10.8}H_{22.9}$). The results of the EXAFS investigation of the solid thus obtained are summarized in Table 2. Hydrolysis of 0.2423 g of this solid with dil. HCl (2.5 mL) gave 0.18 $C_2H_6$, 0.05 $C_2H_4$, and 0.02 $H_2$/Pt. After the aqueous phase had been extracted with toluene and *n*-octane added as the standard, it was analyzed by gas chromatography; found: 0.94 THF and 0.13 *n*-$C_4H_9OH$/Pt.

**Investigation of the reaction product $PtMg_{2.1}Cl_{1.9}C \cdot 2.1$ THF (2), obtained from $PtCl_2$ and $Et_2Mg$ (molar ratio 1:2) in refluxing THF, by means of EXAFS spectroscopy (Table 3, experiment 4):** This experiment has been described in ref. [1a] under experiment 3.1. Both the THF solution and the solid obtained after evaporation of the solution were investigated by the EXAFS method;[12] the results are given in Table 2.

**Preparation of 2 from $PtCl_2$ and EtMgCl (molar ratio 1:4) (Table 3, experiment 5):** The experiment was carried out and analyzed in an analogous manner to that described in ref. [1a] under experiment 3.2. Analysis of the resulting solution of **2** gave $Pt^{2+}$ (4.83 mmol), $Mg^{2+}$ (20.5 mmol), and $Cl^-$ (30.8 mmol).

**Preparation of 2 from $PtCl_2$ and MgA (molar ratio 1:2) (Table 4, experiment 1):** $PtCl_2$ (1.97 g, 7.41 mmol) was added to a stirred suspension of MgA[35] (5.90 g, 14.8 mmol) in THF (155 mL). The mixture was stirred at RT for 5 d. The dark brown solution was filtered (D-4 glass frit), the precipitate washed with THF, and then dried under vacuum to afford a black powder (0.024 g) which contained 7.71% Pt (EA). An aliquot (1.0 mL) was removed from the filtrate (total volume: 280 mL) and was decomposed by addition of a $CH_3OH$/toluene mixture containing *n*-$C_{16}H_{34}$ as the internal standard and subsequently analyzed by gas chromatography. Found: anthracene (A) (13.3 mmol, 89.7%), 9,10-dihydroanthracene (DHA) (0.48 mmol, 3.2%), and *n*-$C_4H_9OH$ [0.80 mmol; 0.11 mol(mol Pt)$^{-1}$]. An aliquot (10.0 mL) of the filtrate was evaporated to dryness under vacuum, and the residue dissolved in [$D_8$]THF. The $^1H$ and $^{13}C$ NMR spectra of this solution showed the presence of free anthracene and the absence of other components. The IR spectrum was recorded as a Nujol suspension of the solid obtained after evaporation of the solvent; it showed the presence of anthracene. An aliquot (5.0 mL) of the filtrate was decomposed by dil. HCl/$H_2O_2$, the THF boiled off and the resulting aqueous solution filtered and analyzed for $Pt^{2+}$ by AAS. Found: $Pt^{2+}$ (7.3 mmol, 98%). An aliquot (10.0 mL) of the filtrate was decomposed by the addition of dil. $H_2SO_4$. Complexometric titration of the aqueous solution at pH = 10 ($Pt^{2+}$ ions were masked by the addition of KCN) gave 14.1 mmol $Mg^{2+}$ and the Volhardt titration gave 15.2 mmol $Cl^-$.

**Preparation of 2 by reaction of $PtCl_2$ with the first and then the second equivalent of MgA (Table 4, experiment 2):** The experiment was conducted analogously to the one described above. After stirring the components in a 1:1 molar ratio for 18 h, a voluminous black precipitate of Pt* (cf. experiment 3.1.) was present. After adding the second equivalent of MgA and stirring for 5 d, only 15 mg of a black solid, containing Pt (17.2%) was isolated on filtration of the solution.

**Active platinum (Pt*) from $PtCl_2$ and MgA (molar ratio 1:1) (Table 5, experiment 1):** A suspension of MgA (4.36 g, 5.98% Mg, 10.7 mmol) in THF (50 mL) was added to a stirred suspension of $PtCl_2$ (2.88 g, 10.8 mmol) in THF (20 mL). The reaction was slightly exothermic reaction and the color of the mixture changed to dark brown. The suspension was stirred at RT for 30 h and then filtered. The precipitated Pt* was washed with THF and dried (high vacuum). Yield: 2.65 g of a black powder of the composition Pt 75.14, Mg 0.52, Cl 2.22, C 18.45, H 1.20% ($PtMg_{0.06}Cl_{0.16}C_{4.0}H_{3.1}$).

A solution obtained by treating Pt* (0.2347 g) with a $CH_3OH$/toluene mixture (containing known amounts of *n*-$C_8H_{18}$ and *n*-$C_{16}H_{34}$ as internal standards) was analyzed by GC. Found: 0.03 A and 0.02 THF/Pt. EXAFS analysis of Pt*: see Figure 2, bottom left and Table 2. Pt* showed no diffraction lines in the XRD spectrum. Broad reflections of Pt appeared in the spectrum after annealing at 400 °C for 24 h. For TEM analysis, Pt* was suspended in EtOH and a small amount of the suspension was applied onto the Cu grid. The TEM images showed crystalline, uniform particles of 3–3.5 nm diameter. According to EDX analyses, the single particles only contain Pt or Pt with small amounts of Cl.



0947-6539/97/0310-1716 $ 17.50+.50/0 *Chem. Eur. J.* **1997**, *3*, No. 10

Table 4. Preparation of **2** from $PtCl_2$ and MgA (molar ratio 1:2).

| Expt | $PtCl_2$ (g) (mmol) | MgA (mmol) | Pt:Mg ratio | THF (mL) | React. $T$ (°C)/ react. $t$ (h) | Solid (g) | Composition of solution | GC of solution (%) A | DHA | $C_4H_9OH$ | NMR | IR |
|---|---|---|---|---|---|---|---|---|---|---|---|---|
| 1 | 1.97 (7.41) | 14.8 | 1:2 | 155 | RT/120 [a] | 0.024 [b] | $PtMg_{1.94}Cl_{2.08}$ | 89.7 | 3.2 | 11 [c] | A | A [d] |
| 2 | 1.93 (7.26) | 7.26 | 1:1 | 120 | 0/ca. 0.25 RT/18 | black precipitate | | | | | | |
| | | 7.21 | 1:1 | | RT/120 [a] | 0.015 | $PtMg_{2.04}Cl_{1.99}$ [e] | 91.2 | 2.1 | 13.4 [c] | | A [d] |

[a] Such a long reaction time is probably not necessary. [b] Pt content: 7.7 %. [c] Mol% of $n$-$C_4H_9OH$/mol Pt. [d] Nujol suspension: in addition to A, absorptions of complexed THF are present in the spectrum. [e] 7.31 mmol of Pt analyzed in the solution.

Table 5. Preparation of Pt* from $PtCl_2$ and MgA (molar ratio 1:1).

| Expt | $PtCl_2$ (g) (mmol) | MgA (mmol) | Pt:Mg ratio | THF (mL) | React. $T$ (°C)/ react. $t$ (h) | Solid (g) | Composition of solid | Investigation of solid | GC of solution A (%) | DHA (%) |
|---|---|---|---|---|---|---|---|---|---|---|
| 1 | 2.88 (10.8) | 10.7 | 1:1 | 70 | RT/30 | 2.65 | $PtMg_{0.06}Cl_{0.16}$-$C_{4.0}H_{3.1}$ [a] | GC [b], EXAFS, XRD, TEM | 81.5 | 2.2 |
| 2 | 2.03 (7.63) | 7.70 | 1:1 | 140 | RT/24 | 1.71 | $PtMg_{0.04}Cl_{0.07}$ [c,d] | GC [b], TEM | 80.1 | 2.2 |

[a] Used for expt 6.1. [b] GC analysis of the solution obtained by alcoholysis. [c] C,H not determined. [d] Used for expt 6.2.

Table 6. Reaction of Pt* with MgA and $MgCl_2$ to produce **2**.

| Expt | Origin of Pt* (Pt content, %) | mmol of Pt used | Pt:MgA:$MgCl_2$ molar ratio | THF (mL) | React. $t$ [a] (h) | Solid (g) | % of A in solution | Investigation of solution |
|---|---|---|---|---|---|---|---|---|
| 1 | expt 5.1 (75.14) | 3.50 | 1:1:1 | 49 | 72 | 0.026 | | EXAFS [b] |
| 2 | expt 5.2 (97.11) | 1.26 | 1:1:1 | 33 | 72 | 0.018 | 90 [c] | |
| 3 | expt 5.1 repeat (81.80) | 2.26 | 1:1.2:1 | 106 | | | Increase of A conc. and decrease of DHA | |
| 4 | Pt black (100) | 2.78 | 1:1:0.83 | 100 | | | conc. in the course of the reactions is presented in Figure 1 | |
| 5 [d] | – | – | –:1:0.85 | 106 | | | | |

[a] At RT. [b] EXAFS of the solid obtained after evaporation of the solvent in vacuum, see Figure 2d and Table 2. [c] GC analysis. [d] Blank experiment in the absence of Pt; same amounts of MgA and $MgCl_2$ used.

Experiment 5.2 was conducted and the products analyzed as described above, except that the precipitate of Pt* was washed with THF *and* pentane. Elemental analysis of Pt* (1.71 g): Pt 97.11, Mg 0.50, Cl 1.24% ($PtMg_{0.04}Cl_{0.07}$). According to GC analysis, Pt contained A (0.02) and THF/Pt (0.01). The TEM image of the Pt* (suspended in EtOH) produced by this experiment, showed crystalline Pt particles ($\approx$3.3 nm).

**EXAFS analysis of 2 produced from Pt*, MgA, and $MgCl_2$ [Eq. (4); Table 6, experiment 1):** A suspension of MgA (3.47 mmol) in THF (40 mL) was added to a stirred suspension of Pt* (0.9092 g) (experiment 5.1; Pt = 3.50 mmol) in THF (9 mL) containing $MgCl_2$ (3.50 mmol). The mixture was stirred at RT for 72 h, the resulting dark brown solution was filtered off (D-4 frit), and the insoluble residue washed with THF and dried under vacuum, to give a black solid (26 mg). The filtrate was evaporated under vacuum and the residue dried under vacuum to yield a black solid (1.36 g): Pt 27.58, Mg 6.69, Cl 9.30, C 42.10, H 4.25% ($PtMg_{1.95}Cl_{1.85}C_{24.8}H_{30.1}$). EXAFS analysis of **2**, see Figure 2, bottom right and Table 2.

**Detection of anthracene liberated in the reaction according to Equation 4 (Table 6, experiment 2):** The experiment was conducted in the same way as the one described above, except that the Pt* used had been produced in experiment 5.2. The reaction time was 72 h. After filtration of the solution, 18 mg of insoluble residue remained. An aliquot of the solution was decomposed by addition of $H_2O$, HCl, and toluene. Analysis of the toluene solution by gas chromatography: A (1.13 mmol, 90%) and DHA (0.12 mmol).

**Investigation of the progression of the reaction according to Equation 4 (Table 6, experiment 3):** Pt* (2.26 mmol) (from a repeat of experiment 5.1; 81.80% Pt), MgA (2.66 mmol), and $MgCl_2$ (2.31 mmol) in THF (106 mL) were stirred at RT for 4 d. At defined time intervals, 1.0 mL samples were removed from the suspension, and 1.0 mL of a $CH_3OH$/toluene mixture containing $n$-$C_{16}H_{34}$ as a standard was added before analysis by GC. In a parallel experiment 6.4, commercial Pt black was used instead of Pt* and a control (experiment 6.5) was carried out in the absence of Pt. The results of experiments 6.3–5 are represented in Figure 1.

**Acknowledgement:** We thank the Fonds der Chemischen Industrie and the PROCOPE program for financial support. We are grateful to the MENESE-CNRS-CEA for access to experimental stations at LURE, and thank Dr. F. Villain, in particular, for her assistance.

Received: March 11, 1997 [F636]

[1] a) L. E. Aleandri, B. Bogdanović, P. Bons, C. Dürr, A. Gaidies, T. Hartwig, S. C. Huckett, M. Lagarden, U. Wilczok, R. A. Brand, *Chem. Mater.* **1995**, *7*, 1153; b) L. E. Aleandri, B. Bogdanović, C. Dürr, D. J. Jones, J. Rozière, U. Wilczok; *Adv. Mater.* **1996**, *8*, 600; c) L. E. Aleandri, B. Bogdanović in *Active Metals* (Ed.: A. Fürstner) VCH, Weinheim, **1996**, pp. 299–338.

[2] Preliminary communication: L. E. Aleandri, B. Bogdanović, C. Dürr, U. Wilczok, D. J. Jones, J. Rozière, *Physica B* **1995**, *208 & 209*, 500.

[3] Preliminary communication: L. E. Aleandri, B. Bogdanović, C. Dürr, M. Lagarden, K. Schlichte, Poster presented at the 24. GDCh Hauptversammlung, Hamburg 5–11 Sept. **1993**; Kurzreferate: AC30, p. 203.

  0947-6539/97/0310-1717 $ 17.50+.50/0 

[4] Instead of $Et_2Mg$, EtMgCl can be used for the preparation of **2**; see Table 3, experiment 5.
[5] Based on the sharpness of these signals, **2** does not appear to be paramagnetic.
[6] The weak signals at $\delta = 0.57$, 0.30, and 0.52 suggest that, as in the reaction of $[Pd(\eta^3\text{-}C_3H_5)_2]$ with $Et_2Mg$ (B. Bogdanović, S. C. Huckett, U. Wilczok, A. Rufinska, *Angew. Chem.* **1988**, *100*, 1569; *Angew. Chem. Int. Ed. Engl.* **1988**, *27*, 1513), organo-bimetallic Pt–Mg complexes could be formed as intermediates.
[7] Lack of $^{195}Pt$ NMR signals in solutions of Pt colloids has been explained by the presence of disordered Pt surfaces which causes strong broadening of resonance lines: J. S. Bradley, J. M. Millar, E. W. Hill, S. Behal, *J. Catal.* **1991**, *129*, 530.
[8] R. Benn, A. Rufinska, *Angew. Chem.* **1986**, *98*, 851; *Angew. Chem. Int. Ed. Engl.* **1986**, *25*, 861.
[9] L. E. Aleandri, B. Bogdanović, A. Gaidies, D. J. Jones, S. Liao, A. Michalowicz, J. Rozière, A. Schott, *J. Organomet. Chem.* **1993**, *459*, 87.
[10] a) T. Yokoyama, S. Kimoto, T. Ohta, *Jap. J. Applied Phys.* **1989**, *28*, L851 b) H. Kuroda, T. Yokoyama, K. Asakura, Y. Iwasawa, *Faraday Discuss.* **1991** *92*, 189. c) L. Tröger, T. Yokoyama, D. Arvanitis, T. Lederer, M. Tischler, K. Baberschke, *Phys. Rev. B.* **1994**, *49*, 888.
[11] M. Lagarden, Dissertation, Bochum University, **1992**.
[12] Also Pt*, after heating to 400 °C, no longer reacts with MgA and $MgCl_2$ in THF: C. Dürr, Dissertation, Bochum University, **1995**.
[13] S. N. Khanna, J. P. Bucher, J. Buttet, F. Cyrot-Lackmann, *Surface Sci.* **1983**, *127*, 165.
[14] C. Solliard, M. Flueli, *Surface Sci.* **1985**, *156*, 487.
[15] N. S. Guyot-Sionnest, F. Villain, D. Bazin, H. Dexpert, F. Le Peltier, J. Lynch, J. P. Bournonville in *X-ray Absorption Fine Structure* (Ed.: S. S. Hasnain), Ellis Horwood, **1991**, pp. 493.
[16] On the basis of a Pt–Pt distance of 2.68 Å and in the fcc structure, it is estimated that the size of the $Pt_{13}$ cluster is 5.4 Å and that of the $Pt_{55}$ cluster is 10.7 Å.
[17] D. G. Duff, P. P. Edwards, J. Evans, J. T. Gauntlett, D. A. Jefferson, B. F. G. Johnson, A. I. Kirkland, D. J. Smith, *Angew. Chem.* **1989**, *101*, 610; *Angew. Chem. Int. Ed. Engl.* **1989**, *28*, 590.
[18] G. Schmid, in: "Structure and Bonding 62—Clusters", 52, Springer-Berlin, **1985**.
[19] B. K. Teo, J. A. Sloane, *Inorg. Chem.* **1985**, *24*, 4545.
[20] B. Moraweck, A. J. Renouprez, *Surface Sci.* **1981**, *106*, 35.
[21] With the program ATOMS, Version 2.44a, B. Ravel, University of Washington.
[22] The centered icosahedron was constructed with 20 tetrahedra of frequency 2, with the edge points of the first shell at $(+/-\iota, +/-1, 0)$, $(0, +/-\iota, +/-1)$, and $(+/-1, 0, +/-\iota)$, and the edge points of the second shell at $(+/-2\iota, +/-2, 0)$, $(0, +/-2\iota, +/-2)$, and $(+/-2, 0, +/-2\iota)$, with $\iota = 1.618034$, giving a distance $R_R = 1.902113f$. Multiplication of all coordinates with a constant factor $f = R_R/1.902113$ leads to the real distances. The coordinates of the atoms in the second shell between the edge points of the tetrahedrons were determined by calculating the position at half distance from both sides. For details see ref. [17], Chart XIII and Chapt. V. The coordinates were not calculated with the formula of the subchapter "Icosahedron".
[23] J. J. Rehr, S. I. Zabinsky, R. C. Albers, *Phys. Rev. Let.* **1992**, *69*, 3397; J. Mustre de Leon, J. J. Rehr, S. I. Zabinsky, R. C. Albers, *Phys. Rev.* **1991**, *B44*, 4146.
[24] J. J. Rehr, *Surface Review Lett.* **1995**, *2*, 63.
[25] The Debye temperature was determined by a fitting procedure without taking account of the contribution from a carbon back-scatterer. Therefore, no further conclusion based on these values should be made. The amplitude-reducing factor *SO* was set to 1.0, RMAX was set to the value of cluster size, the CORRECTION card was not used in the FEFF calculations.
[26] However, a TEM image of isolated Pt* suspended in ethanol showed the presence of much larger, *nanocrystalline* Pt particles (3–3.5 nm diameter) (see Experimental Section and the dissertation cited in ref. [11]; they apparently result from the aggregation of Pt* particles by treatment with ethanol or for other reasons (cf. ref. [7]).
[27] R. Franke, J. Rothe, J. Pollman, J. Hormes, H. Bönnemann, W. Brijoux, T. Hindenburg, *J. Am. Chem. Soc.* **1996**, *118*, 12090.
[28] This idea is supported by the finding (see the dissertation cited in ref. [11]) that, on addition of 1,4-dioxane to a solution of **2** in THF, $MgCl_2$ precipitates out of the solution as insoluble $MgCl_2 \cdot 2C_4H_8O_2$ leaving a soluble system with composition $[PtMg(MgCl_2)_{\approx 0.3}]$. The same phenomenon is also demonstrated by solutions of **1** [1a].
[29] J. S. Bradley, G. H. Via, L. Bonneviot, E. Hill, *Chem. Mater.* **1996**, *8*, 1895 and references therein.
[30] K. J. Klabunde, G. Cardenas-Trivino in *Active Metals* (Ed.: A. Fürstner), VCH, Weinheim, **1996**, pp. 237–278.
[31] O. A. Ferretti, C. Lucas, J. P. Candy, J.-M. Basset, B. Didillon, F. LePeltier, *J. Mol. Catal. A* **1995**, *103*, 125 and references therein.
[32] F. Villain, V. Briois, I. Castro, C. Helary, M. Verdaguer, *Anal. Chem.* **1993**, *65*, 2545.
[33] A. Michalowicz, "EXAFS pour la MAC" in *Société Française de Chimie, Logiciels pour la Chimie* (Paris, **1991**), p. 102–103.
[34] A. G. McKale, *J. Am. Chem. Soc.* **1988**, *110*, 3763.
[35] B. Bogdanović, S. Liao, K. Schlichte, U. Westeppe in *Synthetic Methods of Organometallic and Inorganic Chemistry*, Vol. 1 (Eds.: W. A. Herrmann, A. Salzer), Thieme, Stuttgart, **1996**, p. 43.
[36] B. Bogdanović, B. Spliethoff, *Chem. Ing. Tech.* **1983**, *55*, 156.



0947-6539/97/0310-1718 $ 17.50+.50/0